

Stripes, topological order, and deconfinement in a planar t - J_z model

J. Šmakov^{1,2,3}, C.D. Batista³, and G. Ortiz³

¹*Dept. of Physics and Astronomy, McMaster University, Hamilton, Ontario L8S 4M1, Canada*

²*Condensed Matter Theory, Department of Physics, Royal Institute of Technology–AlbaNova, SE-10691 Stockholm, Sweden*

³*Theoretical Division, Los Alamos National Laboratory, Los Alamos, NM 87545*

(Dated: Received October 29, 2018)

We determine the quantum phase diagram of a two-dimensional bosonic t - J_z model as a function of the lattice anisotropy γ , using a quantum Monte Carlo loop algorithm. We show analytically that the low-energy sectors of the bosonic and the fermionic t - J_z models become equivalent in the limit of small γ . In this limit, the ground state represents a static stripe phase characterized by a non-zero value of a *topological* order parameter. This phase remains up to intermediate values of γ , where there is a quantum phase transition to a phase-segregated state or a homogeneous superfluid with dynamic stripe fluctuations depending on the ratio J_z/t .

PACS numbers: 05.30.-d, 05.70.Fh, 05.30.Jp, 75.10.Jm

During last decade a lot of attention has focused on the study of inhomogeneous structures in strongly correlated materials, such as the copper oxide based high-temperature superconductors (HTSC) [1]. All HTSCs share a common feature – an antiferromagnetic (AF) insulating parent state which evolves into a variety of phases upon doping with carriers, either chemically or using some external probe. In particular, there is experimental evidence [2] that in part of the phase diagram some of these compounds feature inhomogeneous charge and spin textures, commonly known as *stripes*. Existence of such textures is usually justified by competing interactions between the particle constituents, which lead to new locally phase-separated states, all of them characterized by order parameters (OPs) implying that a broken (e.g., translational) symmetry state is in place. The real interest lies in the relation between these stripe phases and superconductivity, since it is unknown how these quantum orders cooperate with or compete against each other [3].

In the present manuscript we argue for the existence of static and dynamic stripe phases in certain (2+1)-dimensional lattice models of strongly correlated materials with no charge-ordered state associated to it, contrary to current understanding. Our starting point is not an assumed system of interacting *stripes* but a system where the latter emerge from the competition between antiferromagnetism and delocalization. We demonstrate that the essential physics is related to the existence of spin antiphase domain structures which are known to be ubiquitous in various doped AF insulators. The t - J_z Hamiltonian is a minimal model for studying that competition which is also present in the t - J model. Particularly, using numerical simulations we determine the quantum phase diagram of a hardcore (HC) bosonic t - J_z planar (2D) model, illustrating the main conclusions of this paper. Our control parameter is the lattice anisotropy γ , $0 \leq \gamma \leq 1$, with $\gamma = 1$ representing the isotropic case with no explicitly broken lattice rotational symmetry [4]. In the small γ regime a confinement interaction *emerges* with a non-vanishing topological hidden order and static incommensurate magnetic orders. This is the static stripe phase which, as the anisotropy is increased, persists up to a critical value γ_c where a confinement-deconfinement transition occurs. At that point the topological stripe order melts and gives way to a phase-segregated state for $J_z > J_z^{c2}$ (for

$\gamma = 1$ see [5]) or to a superfluid phase with static AF correlations and dynamical stripe fluctuations for $J_z^{c2} > J_z > J_z^{c1}$.

There is a number of significant reasons to be interested in this model. First of all, its fermionic counterpart is believed to be a relevant model for electron motion in the copper oxide planes of HTSCs, responsible for unique properties of these materials. Second, we analytically prove that the low-energy spectra of fermionic and bosonic versions of the model are identical in the limit of weak coupling γ between the chains. This is a natural consequence of an exact result in one dimension [6]. Finally, due to the absence of the infamous *fermion sign problem*, we are able to simulate the properties of the model for large lattice sizes and very low temperatures.

We consider a 2D anisotropic t - J_z model on a square lattice for the spin-1/2 HC bosons defined in Ref. [7]

$$H_B = \sum_{i,\nu,\sigma} t^\nu \left(\bar{b}_{i\sigma}^\dagger \bar{b}_{i+e_\nu\sigma} + \text{H.c.} \right) + H_{J_z}, \quad (1)$$

$$H_{J_z} = \sum_{i,\nu} J_z^\nu (S_i^z S_{i+e_\nu}^z - \frac{1}{4} \bar{n}_i \bar{n}_{i+e_\nu}),$$

where vectors $\mathbf{i} = x \mathbf{e}_x + y \mathbf{e}_y$ run over all the N_s sites of a 2D square lattice, \mathbf{e}_ν are the unit vectors of this lattice, and bars over the operators imply that the constraint of no more than one particle per site (the HC constraint) has been already incorporated into the operator algebra. The spin and the number operators on site \mathbf{i} are defined by the following expressions

$$S_i^z = \frac{1}{2} (\bar{n}_{i\uparrow} - \bar{n}_{i\downarrow}) \quad \text{and} \quad \bar{n}_i = \bar{n}_{i\uparrow} + \bar{n}_{i\downarrow}, \quad (2)$$

with $\bar{n}_{i\sigma} = \bar{b}_{i\sigma}^\dagger \bar{b}_{i\sigma}$. Our constrained HC boson operators can be expressed in terms of standard HC boson operators, $b_{i\sigma}^\dagger, b_{j\sigma'}$, which are HC in each flavor and obey the commutation relations: $[b_{i\sigma}, b_{j\sigma'}] = [b_{i\sigma}^\dagger, b_{j\sigma'}^\dagger] = 0, [b_{i\sigma}, b_{j\sigma'}^\dagger] = \delta_{ij} \delta_{\sigma\sigma'} (1 - 2n_{i\sigma})$. The connection between the two bosonic algebras is given by $\bar{b}_{i\sigma}^\dagger = b_{i\sigma}^\dagger (1 - n_{i\bar{\sigma}})$, where $\bar{\sigma}$ denotes the spin orientation opposite to σ . From this expression we can derive the commutators for the algebra which defines our spin-1/2 HC bosons

$$[\bar{b}_{i\sigma}, \bar{b}_{j\sigma'}^\dagger] = \begin{cases} \delta_{ij} (1 - 2\bar{n}_{i\sigma} - \bar{n}_{i\bar{\sigma}}) & \text{for } \sigma = \sigma', \\ -\delta_{ij} \bar{b}_{i\sigma}^\dagger \bar{b}_{i\sigma} & \text{for } \sigma \neq \sigma'. \end{cases} \quad (3)$$

Using the general transformations introduced in Refs. [8, 9], we can map these particles into the HC-constrained fermion operators, $\bar{c}_{i\sigma}^\dagger = c_{i\sigma}^\dagger(1 - n_{i\bar{\sigma}})$ and $\bar{c}_{i\sigma} = (1 - n_{i\bar{\sigma}})c_{i\sigma}$

$$\bar{c}_{i\sigma}^\dagger = \bar{b}_{i\sigma}^\dagger K_i^\dagger, \quad K_i^\dagger = \exp[-i \sum_{\mathbf{j}} \omega(\mathbf{j}, \mathbf{i}) \bar{n}_{\mathbf{j}}]. \quad (4)$$

Here, $\omega(\mathbf{j}, \mathbf{i})$ is the angle between the spatial vector $\mathbf{j} - \mathbf{i}$ and a fixed direction on the lattice. Given this transformation, H_B may be rewritten in terms of the fermionic operators

$$H_B = \sum_{\mathbf{i}, \nu, \sigma} t^\nu \left(\bar{c}_{i\sigma}^\dagger e^{iA_\nu(\mathbf{i})} \bar{c}_{\mathbf{i}+\mathbf{e}_\nu \sigma} + \text{H.c.} \right) + H_{J_z}, \quad (5)$$

with $A_\nu(\mathbf{i}) = \sum_{\mathbf{k}} [\omega(\mathbf{k}, \mathbf{i}) - \omega(\mathbf{k}, \mathbf{i} + \mathbf{e}_\nu)] \bar{n}_{\mathbf{k}}$. Expressions (1) and (5) for H_B only differ in the kinetic-energy term, with the fermionic language including a non-local gauge field $A_\nu(\mathbf{i})$ associated with the change in particle exchange statistics. In general, this gauge field cannot be eliminated in dimensions larger than one which means that different particle statistics can give rise to different physics. However, we will see below that the gauge field is irrelevant and can be eliminated for the low energy spectrum of H_B in the strongly anisotropic region $|t^y| \ll |t^x|$. Notice that t^y can be finite and therefore the problem is still 2D. In other words, when the ratio $\gamma = |t^y|/|t^x|$ is small the properties of the bosonic model governed by the low-energy spectrum of H_B will be identical to the corresponding properties of the fermionic t - J_z model [$H_F = H_B(A_\nu(\mathbf{i}) = \mathbf{0})$].

Let us start by considering the limit $t^y = 0$. In this limit, the system is an array of one-dimensional (1D) t - J_z chains which are only magnetically coupled through J_z^y . From the quasi-exact solution of the 1D t - J_z model [6], it is known that the lowest energy subspace \mathcal{M}_0 consists of states in which the spins are antiferromagnetically ordered and each hole is an antiphase domain for the Néel OP (see Fig. 1a). Since the excited subspaces containing an extra spin excitation are separated by a finite energy gap, \mathcal{M}_0 becomes the relevant subspace to describe the low-energy physics of weakly coupled chains. The combination of the interchain magnetic coupling and the fact that each charge is an antiphase domain gives rise to a confining interaction between holes on adjacent chains. This is because the misalignment of holes on the neighboring chains either breaks the AF bonds or introduces ferromagnetic links, both energetically unfavorable (Fig. 1b). The slope of the linear potential is proportional to $J_z^y = \gamma J_z^x$. This confining interaction leads to a formation of a hole stripe, which is simultaneously a 2D antiphase domain boundary for the Néel OP [10]. Note that the characteristic length of stripe fluctuations is $\ell \sim \gamma^{-1/3}$. For finite hole densities, ρ_h , the stability condition for the existence of a stripe phase is $\gamma \gtrsim \rho_h^3 t^x / J_z^x$.

What happens when a small hopping $t^y \ll t^x$, J_z^x is included? As shown in Fig. 1c, the hopping of the hole to the adjacent chain has an energy cost of $J_z^x/2$. Since $t^y \ll J_z^x$, the magnetic structure again acts as a potential barrier confining the hole to move in the x -direction. The main effect of t^y is a second-order diagonal correction, $2(t^y)^2/J_z^x$ (see Fig. 1c), to the energy of the hole. In other words, the low-energy effective model for $t^y \ll t^x$, J_z^x is essentially the same as the

one for $t^y = 0$. Consequently, the low-energy spectra of the bosonic and the fermionic t - J_z Hamiltonians are the same for $t^y \ll t^x$, J_z^x , i.e., the gauge field of Eq. (5) can be eliminated at low energies because the hole is effectively moving in the x -direction (the transmutator of statistics K_j^\dagger is a symmetry of H_B restricted to its low-energy sector). This concludes the proof of the equivalence of the low-energy spectra of bosonic and fermionic 2D t - J_z models in the strongly anisotropic case.

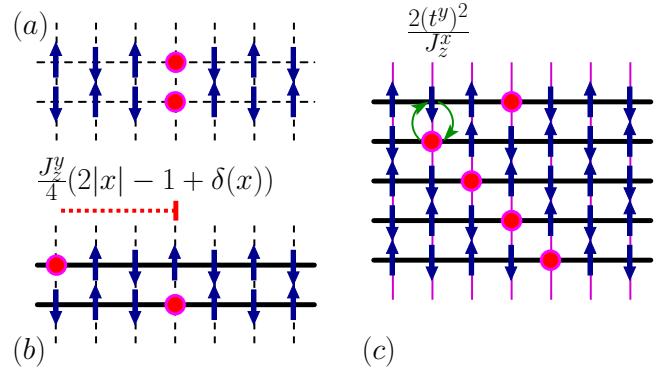


FIG. 1: Illustration of the intrinsic stripe formation mechanism in the 2D anisotropic t - J_z model (a), and energy costs associated with different processes: intra-chain hopping (b) and inter-chain hopping (c). Dynamical confinement emerges from the competition between magnetism and delocalization.

Since a model defined by the Hamiltonian (1) is bosonic, its quantum Monte Carlo (QMC) simulation is not affected by the *sign problem*. We have used the worldline loop algorithm in the continuous imaginary-time formulation (for a review see [11]), similar to the one used for the t - J model in Ref. [12]. This efficient method allows one to perform calculations at very low temperatures and large lattice sizes. Unless noted, all simulations were performed on square lattices of linear size L ranging from 10 to 40, with $\rho_h = 0.2$, and error bars smaller than the size of the symbols. The anisotropy was parameterized by setting $|t^x| = 1$ (all other energy parameters are measured in units of $|t^x|$) and introducing a single parameter $\gamma = |t^y| = J_z^y/J_z^x$, which may vary between zero (disconnected chains) and unity (isotropic 2D model [5]). Temperature was fixed by putting $\beta \equiv |t^x|/(k_B T) = 50$, which was low enough to sample essentially the properties of the ground state. The method is *exact* up to a statistical error and we are using *periodic* boundary conditions to avoid the artificial oscillations introduced by open boundaries [13].

What observable quantities characterize a stripe phase? As argued above one needs to measure both the magnetic structure factor (MSF) and a topological hidden order to uniquely determine it. The MSF ($N_s = L^2$)

$$S(\mathbf{k}) = \frac{4}{N_s} \sum_{\mathbf{i}, \mathbf{j}} e^{i\mathbf{k} \cdot (\mathbf{i} - \mathbf{j})} \langle S_{\mathbf{i}}^z S_{\mathbf{j}}^z \rangle, \quad (6)$$

is expected to display incommensurate peaks at wavevectors $\mathbf{k} = \mathbf{Q} \pm (\pi\delta, 0)$ in the presence of stripes oriented along the y -direction (across the chains), reflecting the 2D character

of the new antiphase boundaries (see Fig. 1c). Here $\mathbf{Q} = (\pi, \pi)$ is the AF wavevector. The results for the AF OP are presented in Fig. 2 for $J_z^x = 1$. For small values of γ , $\gamma = 0.2$ and $\gamma = 0.4$, there are pronounced peaks at wavevectors $\mathbf{k} = (\pi \pm \pi/5, \pi)$ indicating a superstructure with a period of ten lattice spacings, consistent with incommensurate spin ordering and a stripe-like phase. At $\gamma = 0.6$ the height of the incommensurate peaks drops while, simultaneously, the peak at $\mathbf{k} = \mathbf{Q}$ starts to grow, and becomes dominant for $\gamma = 0.8$, signaling a commensurate AF spin ordering.

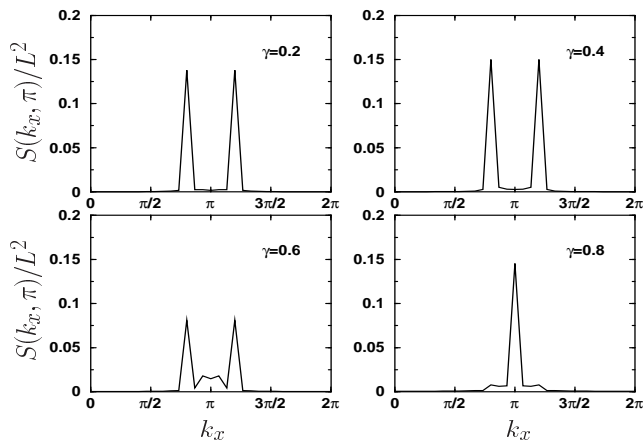


FIG. 2: MSF $S(\mathbf{k})$ for a 30×30 system at hole doping $\rho_h = 0.2$, $J_z^x = 1$, and different values of anisotropy γ . Error bars have been omitted for clarity, standard relative error for any data point never exceeds 10%.

The presence of incommensurate peaks in $S(\mathbf{k})$ does not unequivocally prove the existence of a stripe phase since a similar behavior can be obtained, for example, for a spin spiral phase. It is therefore crucial for our analysis to define another quantity which unambiguously signals the presence of stripes. Since stripes are topological defects (antiphase boundaries), this quantity is called topological OP (TOP) [14] and is calculated for every 1D chain with fixed y coordinate. The corresponding two-point correlation function is

$$G(y) = \frac{4}{N_p^2} \sum_{x, x'=0}^{L-1} \left\langle e^{i\pi T(x, x', y)} S_{(x, y)}^z S_{(x+x', y)}^z \right\rangle, \quad (7)$$

where $S_{(x, y)}^z$ is the spin projection operator at site $\mathbf{i} = x \mathbf{e}_x + y \mathbf{e}_y$, and $N_p = L(1 - \rho_h)$ is the number of particles in the chain. In a system with periodic boundary conditions Eq. (7) is, of course, independent of y , allowing us to average the results of TOP measurements for different chains. The parameter $T(x, x', y)$ is defined by $T(x, x', y) = x' + \sum_{p=0}^{x'} (1 - \bar{n}_{(x+p, y)})$. Without the second term this parameter would just turn Eq. (7) into the square of the 1D Néel OP. The second term, however, introduces an additional factor of (-1) for every hole encountered between the positions x and x' in the chain with fixed coordinate y , indicating that the hole is an antiphase boundary for the Néel OP. It can be easily established that the TOP defined by (7) will reach its

maximum value of unity when evaluated in the ground state of the 1D t - J_z model. Thus, $G(y)$ quantitatively measures to what extent the separate chains in the 2D system have retained their characteristic 1D ground state topological features. A non-vanishing TOP *and* incommensurate spin ordering in the MSF constitute strong evidence that the system is in the stripe phase.

In order to rule out the possibility that the observed behavior is a finite-size effect, we have extrapolated the values of the MSF at the position of the incommensurate peak (Fig. 3) and TOP (Fig. 4) for small values of γ to the infinite system size. Both quantities clearly tend to finite values in the ther-

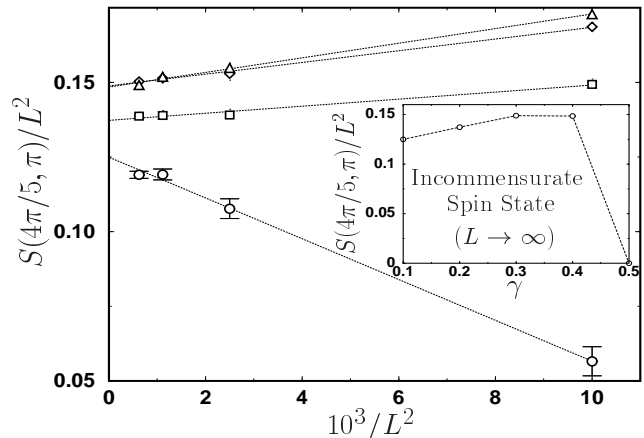


FIG. 3: Finite-size scaling of the MSF $S(\mathbf{k})$ at the position of the incommensurate peak $\mathbf{k} = (4\pi/5, \pi)$ for $J_z^x = 1$ and different values of the anisotropy γ : 0.1 (circles), 0.2 (squares), 0.3 (diamonds), 0.4 (triangles). Lines are linear fits to the QMC data. Data points in the inset are obtained by extrapolation to the $L \rightarrow \infty$ limit, with the dashed line used as a guide to the eye.

modynamic, $L \rightarrow \infty$, limit for the range of γ studied. It is noteworthy, that for the same γ range the value of the MSF at the AF wavevector \mathbf{Q} extrapolates reliably to zero (within error bars).

The non-uniform behavior of the incommensurate peak height (inset of Fig. 3) is a consequence of two competing processes. A stronger coupling between chains leads to a stronger confining potential, facilitating the formation of stripes. On the other hand, the same increase tends to disturb the 1D ground state of the chains due to inter-chain hopping and interactions, driving the system away from stripe ordering. This competition leads to an optimum value $\gamma_0 \sim 0.3$, for which the peak height reaches its maximum.

At $\gamma = \gamma_c$ (see Fig. 5), both the TOP and the incommensurate peak in $S(\mathbf{k})$ extrapolate to zero in the thermodynamic limit. For $\gamma > \gamma_c$, we observe nonzero values of the superfluid density ρ_s with dominant AF correlations if $J_z^x > J_z^{c1}$ (for $J_z^x < J_z^{c1}$ the system is in the Nagaoka ferromagnetic superfluid state). ρ_s was calculated in a 10×10 cluster by computing the mean square deviation of the spatial winding number [15]. Coexistence of AF correlations and superfluidity indicates that the bosons could be moving in pairs since the propagation of individual bosons destroys the AF order-

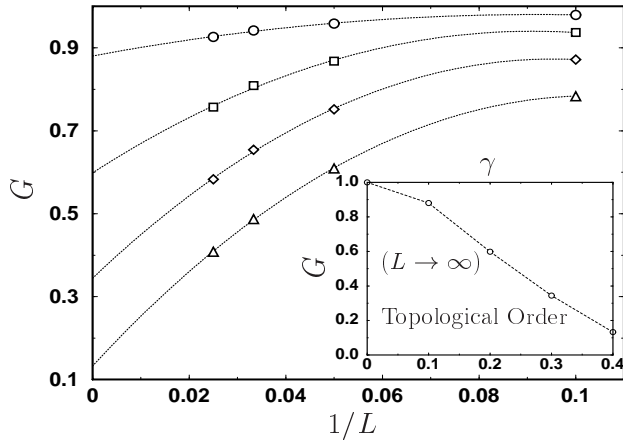


FIG. 4: Finite-size scaling of the TOP G for $J_z^x = 1$ and different values of the anisotropy γ : 0.1 (circles), 0.2 (squares), 0.3 (diamonds) and 0.4 (triangles). Lines are second-order polynomial fits to the QMC data. Data points in the inset are obtained by extrapolation to the $L \rightarrow \infty$ limit, with the dashed line used as a guide to the eye.

ing. For $J_z^x > J_z^{c2} \sim 0.5$, there is a quantum phase transition to a phase-segregated state where a hole-rich superfluid phase coexists with an AF region with no holes. This is the origin of the sharp AF peak of Fig. 2 ($\gamma = 0.8$). Most likely, the *glue* that keeps particles together in the hole-rich region is still the confining interaction provided by the magnetic background.

In summary, we have determined the quantum phase dia-

gram of the planar anisotropic bosonic t - J_z model with periodic boundary conditions. For small values of the anisotropy parameter γ and hole doping ρ_h , there is a quantum stripe phase characterized by topological hidden order, and incommensurate peaks at $\mathbf{k} = \mathbf{Q} \pm (\pi\delta, 0)$ in the MSF. The stripes are formed in the absence of any physical long-range interactions. The glue stabilizing each stripe is a confining potential that emerges dynamically out of the competition between the kinetic energy and the AF exchange. For anisotropies $\gamma > \gamma_c$ a quantum phase transition to a superfluid (deconfining) phase, coexisting with AF correlations, takes place if $J_z^{c2} > J_z^x > J_z^{c1}$. For larger values of J_z^x the system phase segregates. It is remarkable that the same attractive interaction gives rise to both the stripe phase and phase segregation. The existence of a transition between a superfluid and a phase-separated state in proximity of the stripe instability is very suggestive when compared with the phenomenology of the HTSC. The phase-separated region must survive under a transmutation of the statistics because the fermionic kinetic energy is always higher than the bosonic one. The presence of an attractive interaction that segregates the fermions can easily induce a superconducting state if J_z^x is lower but close to the critical value that leads to the phase-segregated state. Note that for the bosonic case, this critical value ($J_z^{c2} \sim 0.5$) is slightly larger than the values of J_z^x that are considered realistic for the cuprate HTSC.

J.Š. is grateful to the Swedish Foundation for Strategic Research, Swedish Research Council, Göran Gustafsson Foundation, SNAC, and SHARCNET.

-
- [1] J. Zaanen and O. Gunnarsson, Phys. Rev. B **40**, 7391 (1989); K. Machida, Physica C **158**, 192 (1989).
 - [2] J.M. Tranquada *et al.*, Nature **375**, 561 (1995).
 - [3] C. D. Batista, G. Ortiz and A. V. Balatsky, Phys. Rev. B **64**, 172508 (2001).
 - [4] B. Normand and A. P. Kampf, Phys. Rev. B **64**, 024521 (2001) studied fermionic Hamiltonians for $\gamma \approx 1$.
 - [5] M. Boninsegni, Phys. Rev. Lett. **87**, 087201 (2001).
 - [6] C. D. Batista and G. Ortiz, Phys. Rev. Lett. **85**, 4755 (2000).
 - [7] C. D. Batista, G. Ortiz and J. E. Gubernatis, Phys. Rev. B **65**, 180402 (2002).
 - [8] C. D. Batista and G. Ortiz, Phys. Rev. Lett. **86**, 1082 (2001).
 - [9] C. D. Batista and G. Ortiz, Adv. in Phys. **53**, 1 (2004).
 - [10] J. Zaanen *et al.*, Philos. Mag. **81**, 1485 (2001).
 - [11] H. G. Evertz, Adv. Phys. **52**, 1 (2003).
 - [12] B. Ammon *et al.*, Phys. Rev. B **58**, 4304 (1998).
 - [13] S. R. White and D. J. Scalapino, Phys. Rev. Lett. **80**, 1272 (1998).
 - [14] M. den Nijs and K. Rommelse, Phys. Rev. B **40**, 4709 (1989).
 - [15] E. L. Pollock and D. M. Ceperley, Phys. Rev. B **36**, 8343 (1987); S. Zhang *et al.*, Phys. Rev. Lett. **74**, 1500 (1995).

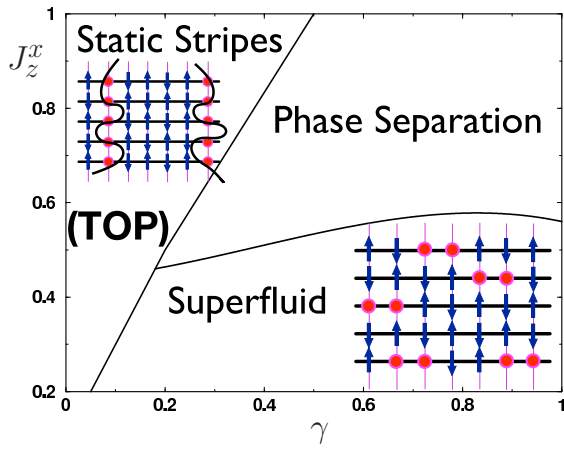


FIG. 5: Quantum phase diagram of the anisotropic bosonic t - J_z model for $\rho_h = 0.2$ ($\rho_h^3 \lesssim \gamma \leq 1$), displaying pictorial representations of the phases.